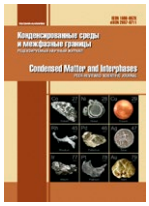

ISSN 1606-867X (Print)
ISSN 2687-0711 (Online)
Condensed Matter and Interphases
Kondensirovannye Sredy i Mezhfaznye Granitsy
https://journals.vsu.ru/kcmf/

Original articles

Research article
https://doi.org/10.17308/kcmf.2023.25/11103

Photosensitising reactive oxygen species with titanium dioxide nanoparticles decorated with PbS quantum dots

A. S. Perepelitsa, S. V. Aslanov, O. V. Ovchinnikov✉, M. S. Smirnov, I. G. Grevtseva, A. N. Latyshev, T. S. Kondratenko

Voronezh State University,
1 Universitetskaya pl., Voronezh, 394018, Russian Federation

Abstract

The development of new efficient photocatalysts based on nanostructured materials with a wide range of photosensitivity in visible and near-infra-red regions and high efficiency of reactive oxygen species generation is an important task. The purpose of this project was to establish the possibility of photosensitising the process of generating reactive oxygen species (ROSs) with TiO_2 nanoparticles (NPs) decorated with colloidal PbS quantum dots (QDs) passivated with 3-mercaptopropionic acid (3MPA) as well as the possibility of increasing the spectral sensitivity of synthesised nanoheterosystems into the red region.

The paper analyses the photocatalytic properties of TiO_2 NPs with an anatase structure and average size of 12 nm decorated with colloidal PbS QDs with an average size of 2.7 nm passivated with 3MPA. It also provides structural and spectral substantiation of the formation of TiO_2 NPs – PbS/3MPA QDs nanoheterostructures. Absorption and luminescence techniques were used to establish the efficiency of generating various ROSs by TiO_2 NPs – PbS/3MPA nanoheterostructures and their individual components under excitation in the UV and visible radiation.

It was shown that TiO_2 NPs decoration with PbS QDs extends the spectral range of sensitivity to the generation of reactive oxygen species in the UV to 1;100 nm. The study revealed an increased efficiency of hydrogen peroxide generation by nanoheterostructures as compared to individual PbS QDs and TiO_2 nanoparticles.

Keywords: Nanoparticles, Titanium dioxide, Quantum dots, Lead sulphide, Photosensitisation, Reactive oxygen species, Photocatalysis

Funding: The study was conducted within the framework of the state order to higher education institutions (FZGU-2023-0007) and the Ministry of Science and Higher Education of the Russian Federation under Agreement (N 075-15-2021-1351).

Acknowledgements: The studies of structural properties conducted by the methods of transmission electron microscopy and X-ray diffractometry were carried out using the equipment of the VSU Centre for Collective Use of Scientific Equipment.

For citation: Perepelitsa A. S., Aslanov S. V., Ovchinnikov O. V., Smirnov M. S., Grevtseva I. G., Latyshev A. N., Kondratenko T. S. Photosensitising reactive oxygen species with titanium dioxide nanoparticles decorated with PbS quantum dots. *Condensed Matter and Interphases*. 2023;25(0): 215–224. https://doi.org/10.17308/kcmf.2023.25/11103

Для цитирования*:* Перепелица А. С., Асланов С. В., Овчинников О. В., Смирнов М. С., Гревцева И. Г., Латышев А. Н., Кондратенко Т. С. Фотосенсибилизация активных форм кислорода наночастицами диоксида титана, декорированными квантовыми точками PbS. Конденсированные среды и межфазные границы. 2023;25(0): 215–224. https://doi.org/10.17308/kcmf.2023.25/11103

✉ Ovchinnikov Oleg Vladimirovich, e-mail: ovchinnikov_o_v@rambler.ru

1. Introduction

The development of effective photocatalysts of various compositions with a wide range of photosensitivity and high efficiency of reactive oxygen species generation is an important scientific and technological task [1]. Traditionally, nanoparticles (NPs) of wide band semiconductors, such as TiO_2, ZnO, ZnS, etc., are used for photocatalysis [1]. However, despite their high photocatalytic activity and stability, they have a number of drawbacks. The key disadvantage of traditional photocatalysts is that they are not photosensitive to the visible and near-infrared spectral regions [1]. Photosensitivity of nanoparticles of wide band semiconductors can be achieved by doping them with non-metal atoms (S, N, C, etc.) and metal ions (Fe^{3+}, Mo^{5+}, Os^{3+}, Rh^{3+}, etc.), hybrid association with molecules of organic dyes, decorating the surface of the NP with plasmonic nanoparticles (Cu, Au, Ag, Pt) or semiconductor colloidal quantum dots (QDs) (Ag_2S, CdSe, etc.) [1–4]. Decoration of the surface of TiO_2 NPs with colloidal QDs of narrow band semiconductors (Ag_2S, PbS, etc.) is of particular interest. PbS is characterised by the narrow band gap and a large Bohr radius of the Wannier–Mott exciton (~18 nm) [5]. These properties allow controlling the position of the exciton absorption peak in the region of 800-2,400 nm [6], and, accordingly, the region of spectral sensitisation of TiO_2 NPs.

[7, 8] demonstrated the possibility of increasing the photocatalytic activity of TiO_2 nanotubes with a size of 90–100 nm when decorating their surface with PbS QDs with a size of 4–5 nm. In this case, PbS nanocrystals were grown directly on the surface of TiO_2 nanotubes. It was shown that decoration of TiO_2 nanotubes increases photocatalytic activity. Other works [9] propose a method for increasing the spectral sensitivity of the TiO_2/Cu heterosystem with a size of ~20 nm by the deposition on their surface of PbS QDs with an average size of 3–5 nm dispersed in toluene. This approach increases the spectral sensitivity of the photocatalyst to 610 nm depending on the size of QDs. However, there have been no systematic descriptions of optical and photocatalytic properties of TiO_2 NPs and PbS QDs heterosystems in literature.

The purpose of this work was to establish the possibility of photosensitisation of ROS in the presence of TiO_2 NPs – PbS/3MPA QDs nanoheterostructures in the visible and near-IR region.

2. Experimental

2.1. Sample synthesis methods

Used reagents are lead nitrate ($Pb(NO_3)_2$), 3-mercaptopropionic acid (3MPA), sodium sulphide (Na_2S), sodium hydroxide (NaOH), 2H-1-benzopyranone-2 (coumarin), imidazole, and 4-nitroso-N,N-dimethylaniline (RNO). They were purchased from Sigma-Aldrich and used without further purification. Amplex UltraRed and horseradish peroxidase were purchased from Thermofisher Scientific.

Colloidal PbS QDs were synthesised in water. 3MPA was used as a passivator. 3MPA (1.5 mmol) was introduced into an aqueous solution of $Pb(NO_3)_2$ (1.5 mmol and 200 ml of water) at 30 °C followed by adjustment of the pH level to 10 with NaOH solution. Then, with constant stirring a peristaltic pump was used to add 50 ml of Na_2S solution (0.8 mmol), which served as a source of sulphur. This ratio of reagents provided for the formation of PbS QDs with a concentration of $6 \cdot 10^{-3}$ mol QD/l in water. To remove the by-products of the reaction, PbS QDs were precipitated with acetone, centrifuged, and redispersed in water.

The resulting PbS QDs were used to form nanoheterostructures with TiO_2 NPs. The experimental technique was similar to the one described in detail in [10, 11]. To form the nanoheterostructures, TiO_2 NPs were dispersed in water and sonicated at 60 kHz until a uniform suspension was obtained. The suspension was then mixed with a QDs solution and dried at room temperature. Free QDs were removed from the resulting grey powder.

2.2. Equipment and experimental techniques

Structural studies of the obtained samples were performed by transmission electron microscopy (TEM) using a Libra 120 PLUS transmission electron microscope (Carl Zeiss, Germany) with an accelerating voltage of 120 kV and a THERMO ARL X'TRA X-ray diffractometer (ThermoFisher, Switzerland).

The optical absorption spectra of the colloidal solution of PbS/3MPA QDs and the diffuse reflection spectra of the powders of TiO_2 –

PbS/3MPA nanoheterostructures were recorded with a USB2000+ spectrometer with the combined USB-DT radiation source and IS80 integrating sphere (Ocean Optics, USA). Barium sulphate powder (P.A.) was used as a white standard to measure diffuse reflection spectra. The absorption coefficient was calculated from the experimental diffuse reflection spectra using the Kubelka-Munk function $F(R)$ [12]:

$$F(R)=\frac{k}{s}=\frac{1-R^2}{2R},$$

where R is the diffuse reflection, k is the absorption coefficient, and s is the scattering coefficient.

A computer-aided spectrometric system based on a MDR-4 diffraction monochromator (LOMO, Russia) with a PDF-10C/M photodiode (ThorLabs, USA) as a radiation receiver were used to record QD luminescence spectra in the range of 800–1,400 nm. An LD PLTB450 semiconductor laser diode (Osram, Germany) with a wavelength of 445 nm and an optical power of 400 mW was used as an excitation source.

Reactive oxygen species were detected by standard absorption and photoluminescence techniques [13]. Production of hydrogen peroxide (H_2O_2) was controlled with an Amplex UltraRed selective sensor [14] in the presence of peroxidase by measuring the rate of luminescence enhancement of the sensor at a wavelength of 596 nm. The concentration of hydroxyl radical (·OH) was determined by the luminescence of 7-hydroxycoumarin (7HC) in the region of 470 nm produced in a coumarin solution in the presence of ·OH radicals [15]. The presence of singlet oxygen ($^1O_2$) was monitored by an absorption method using an imidazole solution with the addition of 4-nitroso-N,N-dimethylaniline (RNO) dye at a ratio of 160:1 to reduce the optical density of the RNO absorption band in the region of 445 nm [16].

3. Results and Discussion

3.1. Structural properties of the studied samples

TEM images demonstrated that ensembles of colloidal PbS QDs had been formed with an average size of nanocrystals of ~2.7 nm and a dispersion in size of ~25% (Fig. 1).

X-ray diffraction analysis of $K_{\alpha 1}$ emission line of copper (1.54 Å) revealed the formation of crystallites, the position of reflexes from which corresponded to the cubic FCC lattice of PbS (*Fmm*) [17] (Fig. 1). Estimates of the average

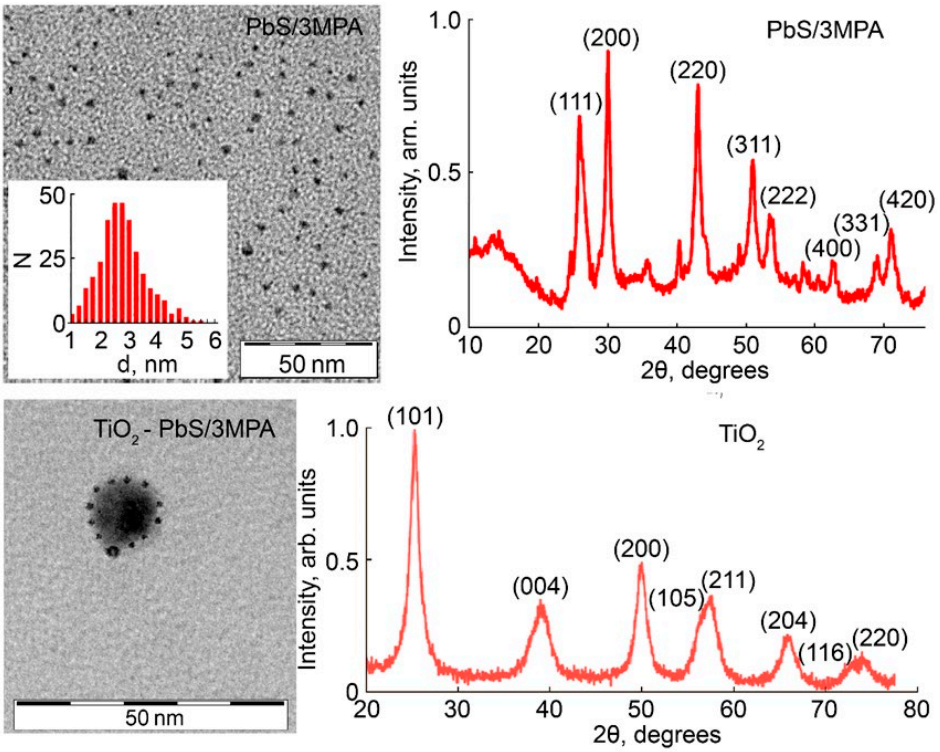

Fig. 1. TEM images and X-ray diffraction patterns of: PbS/3MPA QDs, TiO_2 NPs and TiO_2 – PbS/3MPA nanoheterosystems

size of crystallites performed using the Debye-Scherrer equation [18] had a value of crystallite sizes of ~ 3 nm, which correlated with the TEM data.

X-ray diffraction analysis revealed that TiO_2 NPs had the average size of 12 nm and anatase crystal structure (Fig. 1). TEM images of PbS QDs and TiO_2 NPs mixtures clearly showed nanoparticles with an average size of 10–15 nm on the surface of which there were much smaller NPs with a size of about 2–3 nm (Fig. 1). Comparing the sizes of the detected nanoparticles in mixtures and similar sizes of initial components allows us to assume that the TEM images of mixtures showed TiO_2 NPs with PbS QDs adsorbed on their surfaces.

3.2. Absorption and luminescence properties of the studied samples

The optical absorption spectrum of PbS/3MPA QDs was a broad structureless band with the band edge near 1,300 nm (Fig. 2a) and weak features in the region of 500 and 1,000 nm. The absence of an exciton structure in the PbS QDs optical absorption spectrum can be explained by several factors: 1) size dispersion of QDs, which was detected during the analysis of TEM images; 2) non-stoichiometry of PbS nanocrystals, whose occurrence in PbS nanoscale crystals was indicated in [19]. In this case, optical absorption spectrum for PbS QDs is determined not only by transitions between the quantum size levels in QDs but also by transitions with the participation of trap states.

The intrinsic absorption edge of TiO_2 NPs obtained from the diffuse reflection spectra (Fig. 2a) was located near 3.21 eV and corresponded to the TiO_2 band gap with anatase crystal structure (3.2 eV) [20, 21]. On the long-wavelength side from the intrinsic absorption edge in the region of 3.0–3.2 eV, there was a certain optical density caused by permitted band - trap state transitions. Absorption by trap states in TiO_2 crystals was indicated in [13].

Mixtures of TiO_2 NPs and PbS/3MPA QDs demonstrated transformations of optical absorption spectra. The absorption spectrum of mixtures (Fig. 2a) had a complex structure and was not simply a sum of the spectra of the components. In particular, against the background of strong absorption of TiO_2 NPs (in the quantum energy range above 3.2 eV), there was a broad absorption band in the range of 400–1,100 nm (1–3.1 eV). There were no changes in the absorption region of TiO_2 NPs. Therefore, the transformation of the absorption band structure in the long-wavelength region, for which PbS QDs are accountable in mixtures, and the presence of the absorption band in the region of 200-400 nm, for which TiO_2 NPs are accountable, as well as structural data indicated the formation of TiO_2 NPs – PbS/3MPA nanoheterostructures.

Significant changes were also observed in luminescence when TiO_2 NPs – PbS/3MPA nanoheterostructures were formed. This was accompanied by quenching of PbS QDs luminescence bands in the region of 1,100–

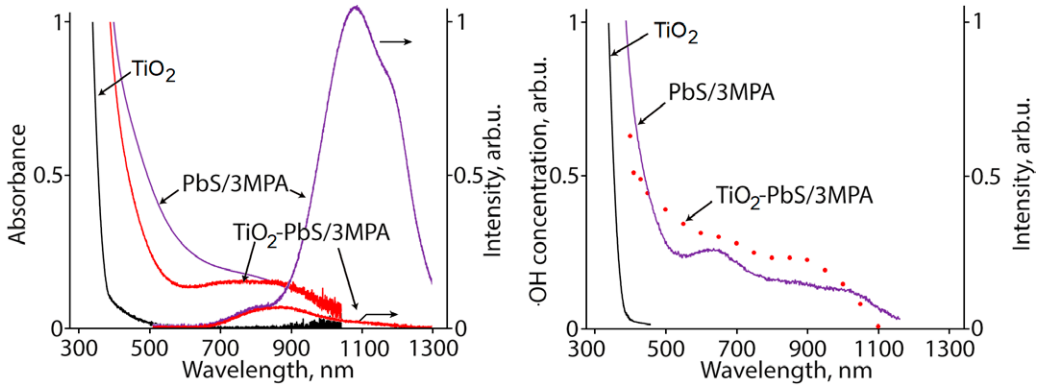

a b

Fig. 2. (a) Optical absorption and photoluminescence spectra of TiO_2, PbS/3MPA QDs, and TiO_2 – PbS/3MPA nano-heterosystems; (b) photoluminescence excitation spectrum of PbS/3MPA QDs and spectral sensitivity dependences of the ·OH radical production in the suspensions of TiO_2 and TiO_2 – PbS/3MPA nano-heterosystems

1,200 nm. A similar pattern was observed in [10, 11] for TiO_2 NPs decorated with Ag_2S QDs. Quenching of PbS QDs luminescence during their adsorption on the TiO_2 NPs interfaces also indicated that nanoheterostructures had been formed and there had been a transfer of photoexcited charge carriers between the nanostructure components. However, luminescence partially kept in the band with a peak at 890 nm indicated that there was no interaction between PbS QDs with a size of less than 2.5 nm (the smallest) present in the ensembles and surface of TiO_2 NPs, which was due to displacement of the quantum size levels of PbS QDs and states of TiO_2 NPs.

3.3. ROS sensitisation with the obtained samples

Figure 3 shows the results of measurements of ROS generation by TiO_2 NPs – PbS/3MPA QDs nanoheterostructures under excitation by UV radiation and radiation in visible spectral regions. It should be noted that during UV excitation, electrons and holes are generated in both TiO_2 and PbS QDs, while during excitation in the visible range they are mainly generated in PbS QDs. Visible radiation allows establishing that PbS QDs provide for TiO_2 photosensitisation to this range. On the other hand, selective excitation of components helps to specify the mechanisms of photocatalytic reactions in the TiO_2 NPs – PbS/3MPA QDs heterosystems. The used methods of ROS detection showed that singlet oxygen ($^1O_2$), hydroxyl radical (·OH) and hydrogen peroxide (H_2O_2) were generated in TiO_2 NPs suspensions exposed to radiation with a wavelength of 365 nm, which is consistent with the data in [22]. In colloidal solutions of PbS/3MPA QDs, we recorded generation of hydrogen peroxide and singlet oxygen (Fig. 4), which had not been previously recorded for PbS QDs in the literature.

The formation of nanoheterostructures led to a change in the efficiency of generation of all types of ROS. Under UV excitation of TiO_2 NPs decorated with PbS/3MPA QDs, in the absorption region of titanium dioxide the efficiency of generation of hydroxyl ·OH radical decreased by 10%, of singlet oxygen by 40%, and the generation of H_2O_2 increased by 3.5 times relative to pure TiO_2 NPs. The efficiency of singlet oxygen and hydrogen peroxide generation by the created nanoheterosystems under excitation

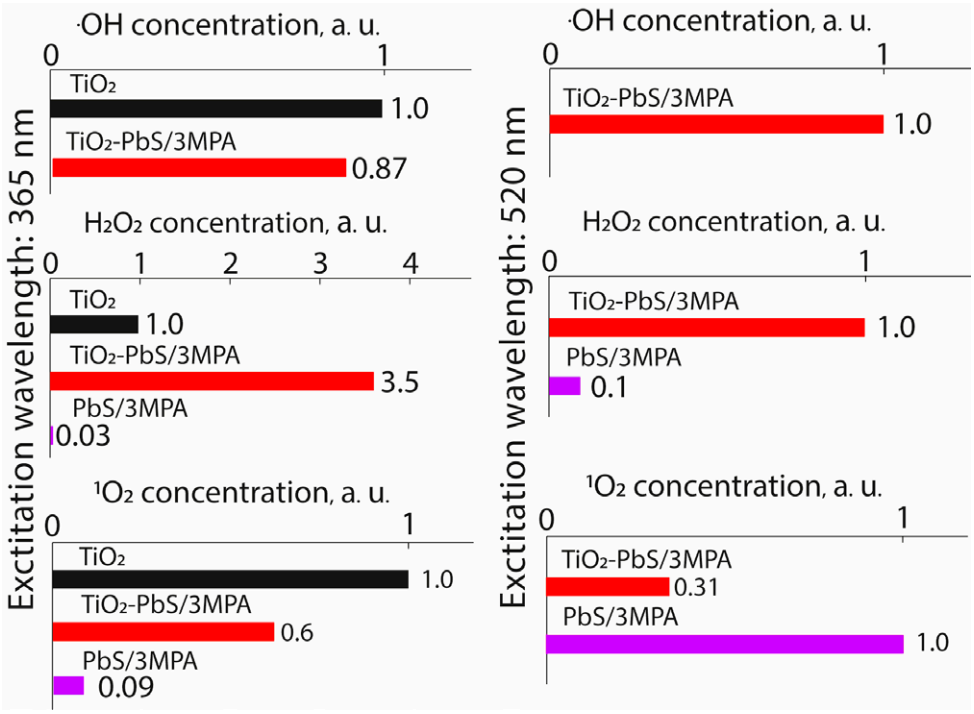

Fig. 3. Histograms of the relative rates of production of hydroxyl radical (·OH), hydrogen peroxide (H_2O_2), and singlet oxygen ($^1O_2$) in the suspensions of TiO_2, PbS/3MPA QDs, and TiO_2 – PbS/3MPA nanoheterosystems when excited by radiation in the UV and visible region of the spectrum

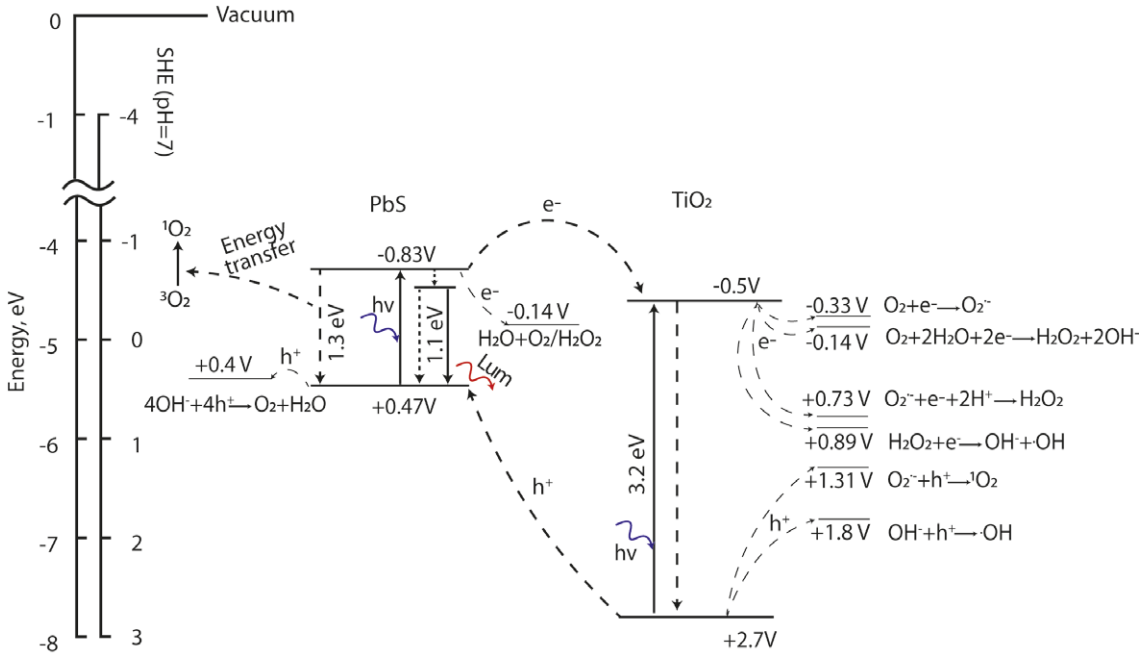

Fig. 4. Scheme of photoprocesses and photocatalytic reactions in the TiO_2 – PbS/3MPA nano-heterosystem. The data on redox potentials and the location of bands were taken from [13, 23-28]

in the UV region of the spectrum increased by 6.6 and 120 times, respectively, relative to pure PbS QDs.

When PbS/3MPA QDs were excited at a wavelength of 520 nm, hydrogen peroxide and singlet oxygen generation was observed. TiO_2 nanoparticles under 520 nm radiation showed no signs of ROS generation. The formation of TiO_2 NPs – PbS/3MPA QDs nanoheterostructures led to the photosensitisation of the ·OH radical, which was not observed in pure PbS QDs, a 10-time increase in hydrogen peroxide generation as compared to the initial PbS/3MPA QDs, and a 3-time decrease in the efficiency of singlet oxygen generation. What is more, for the TiO_2 NPs – PbS/3MPA QDs nanoheterosystems, a broad band of photosensitivity to the generation of ·OH radical was detected in the range from 300 to 1,100 nm, which was absent in case of the initial components (TiO NPs and PbS/3MPA QDs) (Fig. 2b). The shape of the photosensitisation band for ·OH radical qualitatively coincided with the excitation spectrum of PbS/3MPA QDs photoluminescence, which, together with the detected quenching of photoluminescence during the formation of nanoheterostructures, indicated the participation of excitons excited in QDs during ROS generation.

3.4. Empirical model of ROS generation in the studied samples

The obtained results allow justifying in general terms the scheme of the mutual arrangement of the energy levels of PbS/3MPA QDs and TiO_2 NPs (Fig. 4). It should be noted that the generation of ·OH radical and hydrogen peroxide occurred as a result of a charge carrier transfer reaction [13, 23–28]. On the contrary, the production of singlet oxygen was possible both as a result of the transfer of charge carriers and non-radiative energy transfer from the nanoheterosystem (or one of the components) to the molecule of the unexcited triplet oxygen [31]. The formation of TiO_2 NPs – PbS/3MPA QDs nanoheterostructures was accompanied by a pronounced quenching of the PbS QDs luminescence, which was interpreted as the separation of photoexcited charge carriers between the components. Moreover, effective separation of charge carriers was observed both during photoexcitation in the region of strong TiO_2 absorption (UV region) and noticeable PbS QDs absorption (520 nm). Also, the efficiency of ROS production by TiO_2 – PbS/3MPA nanoheterostructures redistributed. It is noteworthy that when a nanoheterosystem was photoexcited in the PbS QDs absorption region (520 nm) an ·OH radical was effectively

produced, which indicated the formation of charge phototransfer channels between the components of the system. Indeed, the comparison of the energy of electron affinity for TiO_2 NPs and PbS QDs (taking into account the size effect for the electron and hole levels) allowed us to assume that a second type heterosystem had been formed, i.e. the quantum-size conduction states for PbS QDs were above the bottom of the TiO_2 NPs conduction band. In this case, the most likely was the phototransfer of electrons from PbS QDs to TiO_2 NPs into the conduction band. Then, the holes remained localised in PbS QDs, which blocked the recombination of charge carriers and facilitated their participation in catalytic reactions of ROS generation.

In this case, the electrons in TiO_2 NPs could react with adsorbed H_2O and O_2 molecules, produce the hydroxyl radical ·OH and hydrogen peroxide H_2O_2. The reaction for the production of hydrogen peroxide is known: $O_2 + 2e^- + 2H^+ \rightarrow H_2O_2$. This reaction requires a photoelectron from the TiO_2 conduction band [13, 23–28]. In this case, the formation of a heterosystem should contribute to an increase in the efficiency of H_2O_2 generation both when excited in the UV and visible region, which was observed during the experiment. The generation of the ·OH radical in the presence of TiO_2 can be provided for by two reactions: both with the participation of electrons from the conduction band (1) $TiO_2 - H_2O_2 + e^- \rightarrow \cdot OH + OH^-$ [13, 23–28] and holes from the valence band (2) TiO_2 (2) $OH^- + h^+ \rightarrow \cdot OH$. Separation of charge carriers in the heterosystem contributes to the hole localisation in PbS, which blocks reaction (2). In this case, the efficiency of the ·OH radical generation during the heterosystem formation may decrease, which was observed during the experiment under excitation in the UV region. Under the influence of visible radiation, the electron and ~~the~~ hole are generated in PbS QDs. The mutual arrangement of PbS QDs and TiO_2 NPs levels contributes to the transition of the electron to the TiO_2 conduction band. This photo-excited electron from the TiO_2 conduction band can participate in the generation of the ·OH radical by reaction (1). Indeed, under the influence of visible radiation the generation of the ·OH radical was detected for heterosystems, which is not characteristic of individual components. To close the proposed scheme of the ·OH radical generation under the influence of visible radiation and to let the photocatalyst operate for an unlimited time, reduction of PbS QDs is needed. The study revealed that the generation of the ·OH radical under the influence of visible radiation is not saturated. However, so far the mechanism of PbS QDs reduction has not been established and will be studied separately.

As have been noted, the generation of singlet oxygen is possible both as a result of the charge carrier transfer (electron and hole) and ~~the~~ non-radiative energy transfer from the nanoheterosystem (or one of the components) to the molecule of unexcited triplet oxygen [23–28, 30, 31]. In the case of UV excitation of TiO_2, the following two-stage process is recognised as the main mechanism: (3) $O_2 + e \rightarrow O_2^{\bullet -}$ and (4) $O_2^{\bullet -} + h^+ \rightarrow {}^1O_2$ [13, 27]. The process of singlet oxygen generation in PbS QDs detected by us cannot proceed by reaction (4) in terms of energy since the level of size quantisation for holes in PbS QDs is located above the oxidative potential $O_2^{\bullet -}/{}^1O_2$. Therefore, the only possible mechanism is the exchange-resonance mechanism of non-radiative transfer of excitation energy from PbS QDs to ${}^3O_2$ and excitation of the latter to the singlet state of ${}^1O_2$. This scheme was indirectly confirmed by a sharp decrease in the efficiency of ${}^1O_2$ generation in TiO_2 NPs (UV excitation) when introducing a hole acceptor into the solution, which blocked reaction (4). Introduction of a hole acceptor to the PbS QDs did not change the rate of ${}^1O_2$ generation. In heterosystems, a decrease in the rate of ${}^1O_2$ generation under excitation in the visible radiation as compared to pure PbS QDs is determined by the effective separation of charge carriers between components. It should be noted that we did not find any reports of ${}^1O_2$ photogeneration in PbS QDs. This was observed for carbon, CdS, and ZnS QDs [30, 31].

4. Conclusions

The authors developed a method for decorating the surface of TiO_2 NPs with colloidal PbS QDs with an average size of 2.7 nm obtained in an aqueous solution of 3-mercaptopropionic acid. The following spectral manifestations of the formation of the TiO_2 – PbS/3MPA nanoheterosystem were detected: i) in terms of absorption properties

the study revealed a transformation of PbS QDs absorption bands during adsorption to the surface of TiO_2 NPs; ii) there was quenching of PbS QDs luminescence in the region of 1000-1400 nm during the formation of the TiO_2 – PbS/3MPA QDs nanoheterosystems. Studies were conducted to check the possibility of generating ROS by the obtained nanoheterosystems. The generation of singlet oxygen and hydrogen peroxide in the presence of PbS QDs was detected. It was shown that decorating the surface of TiO_2 NPs resulted in a 10% decrease in the efficiency of hydroxyl radical generation, and a 40% decrease in the efficiency of singlet oxygen generation as compared to pure TiO_2 NPs. The rate of hydrogen peroxide generation increased up to 3.5 times relative to the TiO_2 NPs and up to 150 times relative to PbS/3MPA QDs under excitation by UV radiation. The generation of ROS was detected when excited by radiation in the visible spectrum, which was absent in case of pure TiO_2 NPs. It was determined that the generation of hydrogen peroxide increased by 10 times and the production of singlet oxygen decreased by 3 times relative to pure PbS QDs. The study revealed hydroxyl radical sensitisation absent in case of pure PbS QDs. It also established an expansion of the excitation region of ROS production to 1100 nm. An empirical model for photoprocesses in the studied nanoheterosystems was created.

Author contributions

A. S. Perepelitsa: conducting scientific research, writing of the article, scientific editing of the text; S. V. Aslanov: conducting scientific research, scientific editing of the text; O. V. Ovchinnikov: head of scientific research, scientific editing of the text, discussion of the results of the study; M. S. Smirnov: scientific editing of the text, discussion of the results of the study; I. G. Grevtseva: scientific editing of the text, discussion of the results of the study; A. N. Latyshev: scientific editing of the text, discussion of the results of the study; T. S. Kondratenko: scientific editing of the text, discussion of the results of the study.

Conflict of interests

The authors declare that they have no known competing financial interests or personal relationships that could have influenced the work reported in this paper.

References

1. *Micro and nano technologies, nanotechnology and photocatalysis for environmental applications*. M. Tahir, M. Rafique, M. Rafique (eds.). Amsterdam: Elsevier Inc. 2020. 244 p.

2. Huang F., Yan A., Zhao H. Influences of doping on photocatalytic properties of TiO_2 photocatalyst. In: *Semiconductor photocatalysis - materials, mechanisms and applications*. https://doi.org/10.5772/63234

3. Li R., Li T., Zhou Q. Impact of titanium dioxide (TiO_2) modification on its application to pollution treatment – a review. *Catalysts*. 2020;10(7): 804. https://doi.org/10.3390/catal10070804

4. Janczarek M., Kowalska E. On the origin of enhanced photocatalytic activity of copper-modified titania in the oxidative reaction systems. *Catalysts*. 2017;7(11): 317. https://doi.org/10.3390/catal7110317

5. Kang I., Wise F. W. Electronic structure and optical properties of PbS and PbSe quantum dots. *Journal of the Optical Society of America B*. 1997;14:(7): 1632–1646. https://doi.org/10.1364/JOSAB.14.001632

6. Su G., Liu C., Deng Z., Zhao X., Zhou X. Size-dependent photoluminescence of PbS QDs embedded in silicate glasses. *Optical materials express*. 2017;7(7): 2194–2207. https://doi.org/10.1364/OME.7.002194

7. Zhang H., Gao Y., Zhu G., Li B., Gou J., Cheng X. Synthesis of PbS/TiO_2 nano-tubes photoelectrode and its enhanced visible light driven photocatalytic performance and mechanism for purification of 4-chlorobenzoic acid. *Separation and Purification Technology*. 2019;227: 115697. https://doi.org/10.1016/j.seppur.2019.115697

8. Ratanatawanate C., Tao Y., Balkus K. J. Jr. Photocatalytic activity of PbS quantum dot/TiO_2 nanotube composites. *Journal of Physical Chemistry.* C 2009;113(24): 10755–10760. https://doi.org/10.1021/jp903050h

9. Wang C., Thompson R. L., Ohodnicki P., Baltrus J., Matranga C. Size-dependent photocatalytic reduction of CO_2 with PbS quantum dot sensitized TiO_2 heterostructured photocatalysts. *Journal of Materials Chemistry.* 2011;21: 13452. https://doi.org/10.1039/C1JM12367J

10. Ovchinnikov O. V., Smirnov M. S., Aslanov S. V., Perepelitsa A. S. Luminescent properties of colloidal Ag_2S quantum dots for photocatalytic applications. *Physics of the Solid State*. 2022;64(13): 12054–2061. https://doi.org/10.21883/PSS.2022.13.53973.19s

11. Ovchinnikov O. V., Smirnov M. S., Perepelitsa A. S., ... Hussein A. M. H. Photosensitisation of reactive oxygen species with titanium dioxide nanoparticles decorated with silver sulphide quantum dots. *Condensed Matter and Interphases*. 2022;24(4):

511–522. https://doi.org/10.17308/kcmf.2022.24/10555

12. Kubelka P., Munk F. An article on optics of paint layers. *Fuer Tekn. Physik*. 1931;12: 593-609.

13. Nosaka Y., Nosaka A. Y. Generation and detection of reactive oxygen species in photocatalysis. *Chemical Reviews*. 2017;117: 11302–11336. https://doi.org/10.1021/acs.chemrev.7b00161

14. Mohanty J. G., Jaffe J. S., Schulman E. S., Raible D. G. A highly sensitive fluorescent micro-assay of H_2O_2 release from activated human leukocytes using a dihydroxyphenoxazine derivative. *Journal of Immunological Methods*. 1997;202(2): 133–141. https://doi.org/10.1016/S0022-1759(96)00244-X

15. Wafi A., Szabó-Bárdos E., Horváth O., Makó E., Jakab M., Zsirka B. Coumarin-based quantification of hydroxyl radicals and other reactive species generated on excited nitrogen-doped TiO_2. *Journal of Photochemistry and Photobiology A: Chemistry*. 2021;404: 112913. https://doi.org/10.1016/j.jphotochem.2020.112913

16. Herman J., Neal S. L. Efficiency comparison of the imidazole plus RNO method for singlet oxygen detection in biorelevant solvents. *Analytical and Bioanalytical Chemistry*. 2019;411(20): 5287–5296. https://doi.org/10.1007/s00216-019-01910-2

17. Sadovnikov S. I., Kozhevnikova N. S., Pushin V. G., Rempel A. A. Microstructure of nanocrystalline PbS powders and films. *Inorganic Materials*. 2012;48: 21–27. https://doi.org/10.1134/S002016851201013X

18. Gusev A. I. *Nanomaterials, nanostructures, nanotechnologies**. Moscow: Fizmatlit Publ.; 2005. 416 p. (In Russ.)

19. Sadovnikov S. I., Rempel A. A. Nonstoichiometric distribution of sulfur atoms in lead sulfide structure. *Doklady Physical Chemistry*. 2009;428(1): 167–171. https://doi.org/10.1134/S0012501609090024

20. Kapilashrami M., Zhang Y., Liu Y.-S., Hagfeldt A., Guo J. Probing the optical property and electronic structure of TiO_2 nanomaterials for renewable energy applications. *Chemical Review*. 2014;114: 9662–9707. https://doi.org/10.1021/cr5000893

21. Murphy A. B. Band-gap determination from diffuse reflectance measurements of semiconductor films, and application to photoelectrochemical water-splitting. *Solar Energy Materials & Solar Cells*. 2007;91: 1326–1337. https://doi.org/10.1016/j.solmat.2007.05.005

22. Nakata K., Fujishima A. TiO_2 photocatalysis: Design and applications. *Journal of Photochemistry and Photobiology C: Photochemistry Reviews*. 2012;13(3): 169–189. https://doi.org/10.1016/j.jphotochemrev.2012.06.001

23. Athanasekou C. P., Likodimos V., Falaras P. Recent developments of TiO_2 photocatalysis involving advanced oxidation and reduction reactions in water. *Journal of Environmental Chemical Engineering*. 2018;6(6): 7386–7394. https://doi.org/10.1016/j.jece.2018.07.026

24. Turrens J. F. Mitochondrial formation of reactive oxygen species. The Journal of Physiology. 2003;552(2): 335-44. https://doi.org/10.1113/jphysiol.2003.049478

25. Fujishima A., Zhang X., Tryk D. A. TiO_2 photocatalysis and related surface phenomena. *Surface Science Reports*. 2008;63(12): 515–582. https://doi.org/10.1016/j.surfrep.2008.10.001

26. Kohtani S., Yoshioka E., Miyabe H. Photocatalytic hydrogenation on semiconductor particles. In: *Hydrogenation*. I. Karame (ed.). *IntechOpen*. 2012. 340 p. https://doi.org/10.5772/45732

27. Bard A. J., Parsons R., Jordan J. *Standart potentials in aqueous solutions*. Routledge, 1985. 848 p. https://doi.org/10.1201/9780203738764

28. Belovolova L.V. Reactive oxygen species in aqueous media (a review). *Optics and Spectroscopy*. 2020;128: 932–951. https://doi.org/10.1134/S0030400X20070036

29. Segets D., Lucas J. M., Klupp Taylor R. N., Scheele M., Zheng H., Alivisatos A. P., Peukert W. Determination of the quantum dot band gap dependence on particle size from optical absorbance and transmission electron microscopy measurements. *ACS Nano*. 2012,6(10): 9021–9032. https://doi.org/10.1021/nn303130d

30. Ge J., Jia Q., Liu W., ... Wang P. Carbon dots with intristic theranostic properties for bioimaging, red-light-triggered photodynamic/photothermal simultaneous therapy in vitro and in vivo. Advanced Healthcare Materials. 2016;5(6): 665-675. https://doi.org/10.1002/adhm.201500720

31. Bailón-Ruiz S., Perales-Pérez O. J. Generation of singlet oxygen by water-stable CdSe(S) and Znse(S) quantum dots. *Applied Materials Today*. 2017;9: 161-166. https://doi.org/10.1016/j.apmt.2017.06.006

* *Translated by author of the article.*

Information about the authors

Aleksey S. Perepelitsa, Cand. Sci. (Phys.–Math.), Associate Professor at the Department of Optics and Spectroscopy, Voronezh State University (Voronezh, Russian Federation).

https://orcid.org/ 0000-0002-1264-0107

a-perepelitsa@yandex.ru

Sergey V. Aslanov, Cand. Sci. (Phys.–Math.), Lecturer of the Department of Optics and Spectroscopy, Voronezh State University (Voronezh, Russian Federation).

https://orcid.org/0000-0002-3961-2480

windmaster7@yandex.ru

Oleg V. Ovchinnikov, Dr. Sci. (Phys.–Math.), Full Professor, Dean of the Faculty of Physics, Head of the Department of Optics and Spectroscopy, Voronezh State University (Voronezh, Russian Federation).
https://orcid.org/0000-0001-6032-9295
ovchinnikov_o_v@rambler.ru

Mikhail S. Smirnov, Dr. Sci. (Phys.–Math.), Associate Professor, Department of Optics and Spectroscopy, Voronezh State University (Voronezh, Russian Federation).
https://orcid.org/0000-0001-8765-0986
smirnov_m_s@mail.ru

Irina G. Grevtseva, Cand. Sci. (Phys.–Math.), Lecturer at the Department of Optics and Spectroscopy, Voronezh State University (Voronezh, Russian Federation).
https://orcid.org/0000-0002-1964-1233
grevtseva_ig@inbox.ru

Anatoly N. Latyshev, Dr. Sci. (Phys.–Math.), Full Professor, Department of Optics and Spectroscopy, Voronezh State University (Voronezh, Russian Federation).
https://orcid.org/0000-0002-7271-0795
latyshev@phys.vsu.ru

Tamara S. Kondratenko, Dr. Sci. (Phys.–Math.), Associate Professor, Department of Optics and Spectroscopy, Voronezh State University (Voronezh, Russian Federation).
https://orcid.org/0000-0003-4936-0130
tamara-shatskikh@rambler.ru

Received 29.10.2022; approved after reviewing 05.12.2022; accepted for publication 20.12.2022; published online 25.06.2023.

Translated by Irina Charychanskaya
Edited and proofread by Simon Cox